*35th EPS Conference on Plasma Phys. Hersonissos, 9 - 13 June 2008 ECA Vol.**32D**, P-1.019 (2008)*

Avalanche-like bursts in global gyrokinetic simulations

B. F. McMillan[1], S. Jolliet[1], T. M. Tran[1], A. Bottino[2], P. Angelino[3] and L. Villard[1]

[1] *Ecole Polytechnique Fédérale de Lausanne (EPFL), Centre de Recherches en Physique des Plasmas, Association Euratom-Confédération Suisse, 1015 Lausanne, Switzerland.*
[2] *Max Planck Institut fur Plasmaphysik, IPP-EURATOM Association, Garching*
[3] *Association Euratom-CEA, CEA/DSM/DRFC Cadarache, France*

Abstract

Surface and globally averaged heat fluxes can be highly time variable in gyrokinetic simulations. During a burst of turbulence, instantaneous surface averaged fluxes may momentarily reach levels several times higher than their typical (median) levels: the result is that time-averaged flux levels are often considerably larger than typical (median) values. The bursts can in this sense be said to drive a substantial fraction of the transport. Burst-driven fluxes and flows often have long radial correlation lengths, and frequently take the form of radially propagating fronts, or *avalanches*. Given the large radial scale lengths of the bursts, they could play a significant role in non-local transport, and possibly in departures from gyro-Bohm scaling. We explore the characteristics of the bursts and examine how levels of fluctuation in the system depend on parameters like plasma size and gradient scale lengths. One interesting result is that there is a strong relationship between the avalanche properties and time-averaged global flow structures in the simulation. We find that the propagation direction of the avalanches depends on the sign of the shearing rate. We test an explanation for avalanche propagation based on the linear dispersion of waves which have been tilted by sheared flow.

Global gyrokinetic simulations of CYCLONE plasmas using the ORB5 code[1] show bursts in the global flux level; flux plots versus radius and time show inward and outward propagating structures, as do other fluid [2] and gyrokinetic[3] simulations. We present relatively long simulations with $\rho^* = 1/140$ and $\rho^* = 1/280$: figures 1(a) and 1(b) show the flux versus time and radial position for these simulations.

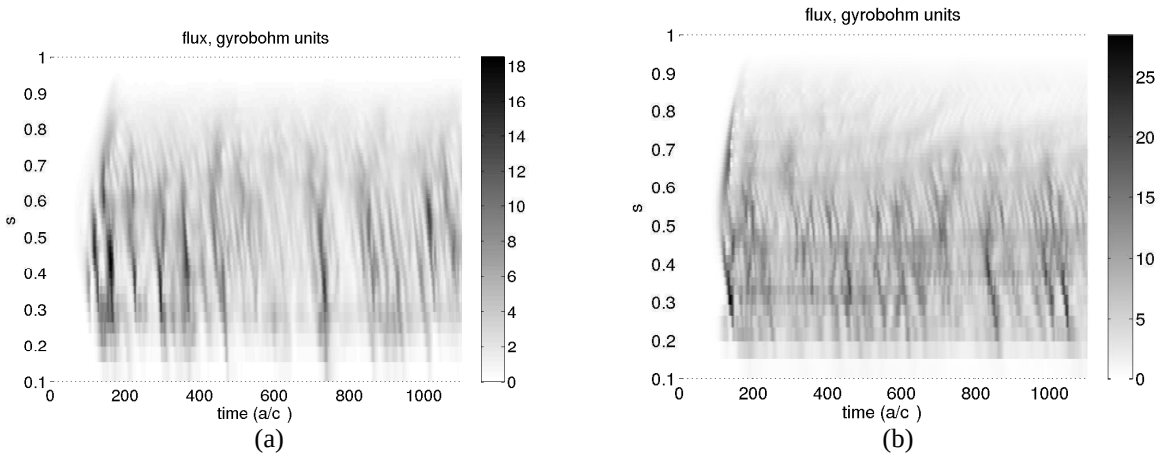

Figure 1: Flux versus radial coordinate (s) and time in a simulation with $\rho^* = 1/140$ (a) and $\rho^* = 1/280$ (b).

The flux plots of the two simulations are qualitatively quite different: in the smaller simulation, global scale zonal flows develop in the simulation at late time, and flux events are

correlated across almost the full width of the simulation domain, whereas in the larger simulation, global scale flows have a relatively small amplitude, and large flux events propagate over only a limited proportion if the plasma radius. We therefore only expect to be in a large system limit, and achieve good scale separation, for $\rho^* \gtrsim 280$. The flux plots show both large and small amplitude propagating features: the propagation speed appears to be independent of amplitude.

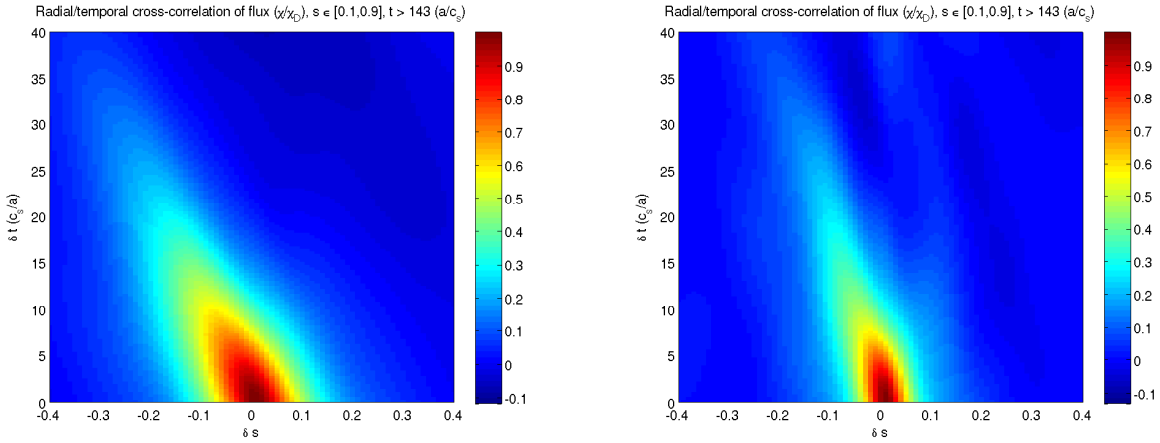

(a) (b)

Figure 2: Autocorrelation of time-varying component of the flux versus spatial and temporal offset, $\rho^* = 1/140$ (a) and $\rho^* = 1/280$ (b).

The 2-D (radial and temporal) autocorrelation of the time-varying component of the flux is plotted in figures 2(a) and 2(b). The magnitude of the correlation is < 0.1 beyond time lags of $50(a/c_s)$. There is a substantial leftward movement of the maximum correlation point at increasing time lags, indicating inward propagating structures. At a time lag of $18(a/c_s)$, the maximum correlation is 0.2, with a radial displacement $\delta s = -0.17$ for $\rho^* = 1/140$ and $\delta s = -0.08$ for $\rho^* = 1/280$. The velocity of the structure is approximately $-1.4\rho^* c_s$, of the same order as the average $E \times B$ velocity. Note that these autocorrelation plots are very similar when radius is measured in units of gyroradius, indicating that these events are local, and do not scale with system size. The most notable difference is that in the larger simulation, evidence for outward-going structures also appears as a tail going toward positive δs at later times, but with lower overall amplitude than the inward-going tail.

These bursty features are also seen clearly in figure 3(a), a plot of the zonally averaged radial electric field in the $\rho^* = 1/280$ simulation. Clear propagating structures are identified, strongly correlated with the bursts of flux: also, vertically aligned structures associated with geodesic acoustic modes (GAMs) can be seen towards the plasma edge $s > 0.7$, at higher frequencies than other features. Because the GAMs have relatively long wavelength, they do not in plots of the shearing rate (figure 3(b)), and are not expected to be able to suppress turbulence by shearing: the bursts we are interested in also have considerably lower frequencies than the GAMs, so it appears that the GAMs do not play a role in burst dynamics. The role of zone boundaries in the dynamics of the bursts is evident in these two figures, where, in the outer region $s \in [0.5 : 0.9]$, the zone boundaries separate inward from outward propagating behaviour. We note that the rapid fluctuations in the shearing rate are of roughly the same size as the quasi-static shear associated with long-lived zonal flows: this suggests that burst driven shear could have a significant back-reaction on the bursts themselves.

We suggest an explanation for the favoured propagation direction for bursts depending on the sign of low frequency component of the shear flow: turbulent eddies, which are generated

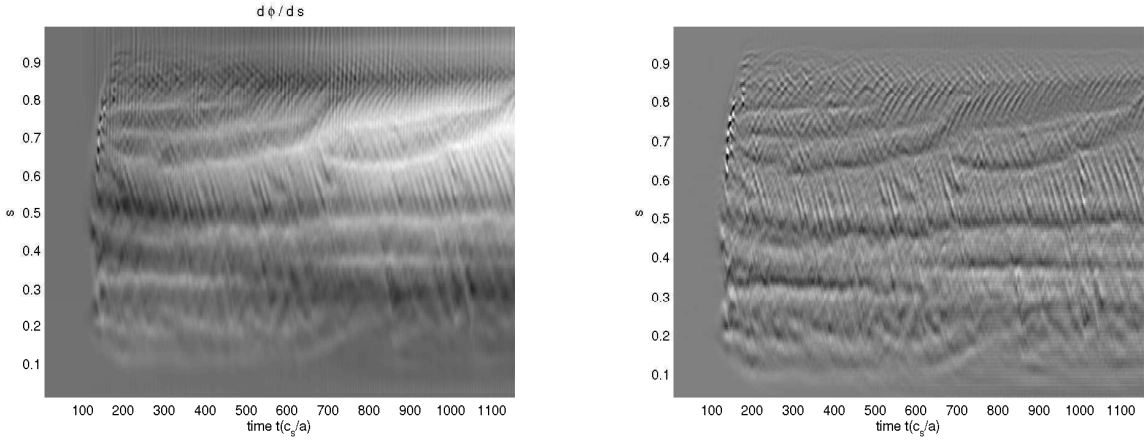

Figure 3: (a) First radial derivative of zonal potential for the $\rho^* = 1/280$ simulation and (b) the second derivative of the zonal potential.

linearly with $k_r \sim 0$, are tilted by the shear, and then propagate radially due to the finite radial group velocity $v_r \sim < d\omega/dk_r >$ for modes with $k_r \neq 0$. The linear mode frequency, determined from a linear flux-tube gyrokinetic simulation (figure 4(a)) using the GENE code[4], shows a quite strong dependence on radial wavenumber for the waves with $k_y\rho_i \in [0.15, 0.3]$, where most of the turbulent spectral energy is concentrated; in the range, and for $k_r \lesssim k_y$, $\partial\omega/\partial k_r = -12.4\rho^* c_s(k_r/k_y)$ is a reasonable fit to the dispersion relation. The average tilt of the turbulence as a function of radius was measured by analysing the potential on the s, ϕ plane: in the $\rho_* = 1/140$ simulation, $k_r/k_\theta > 0$ over most of the domain. The tilting angle of the turbulence is such that $k_r \sim 0.5|k_y|$, and the associated absolute velocity is $6\rho^* c_s$, about four times larger than the burst velocity. The sign of the propagation velocity found in the simulations is in agreement with that predicted from the group velocity propagation mechanism.

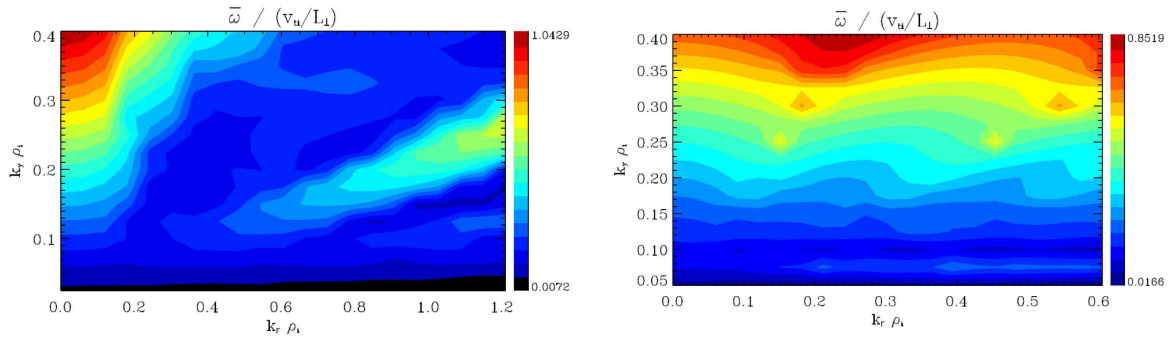

Figure 4: Frequency versus poloidal and radial wavenumber for ITG modes in a flux tube with CYCLONE parameters (a), and in a simulation with magnetic shear reduced by a factor of four.

As a further exploration of the burst mechanism, we consider a test cast with substantially reduced magnetic shear, with more slab-like turbulence. The zonal radial electric field (fig. 5) shows fairly symmetrical inward and outward propagating features overlapping in the same shear zone; typically the features propagate radially over one or two zones. The ITG mode frequency for strongly reduced shear (figure 4(b)) show much weaker dispersion in k_x than for CYCLONE parameters, so no preferred propagation direction is expected, consistent with the simulation results. This also demonstrates that the burst propagation mechanism is not solely ra-

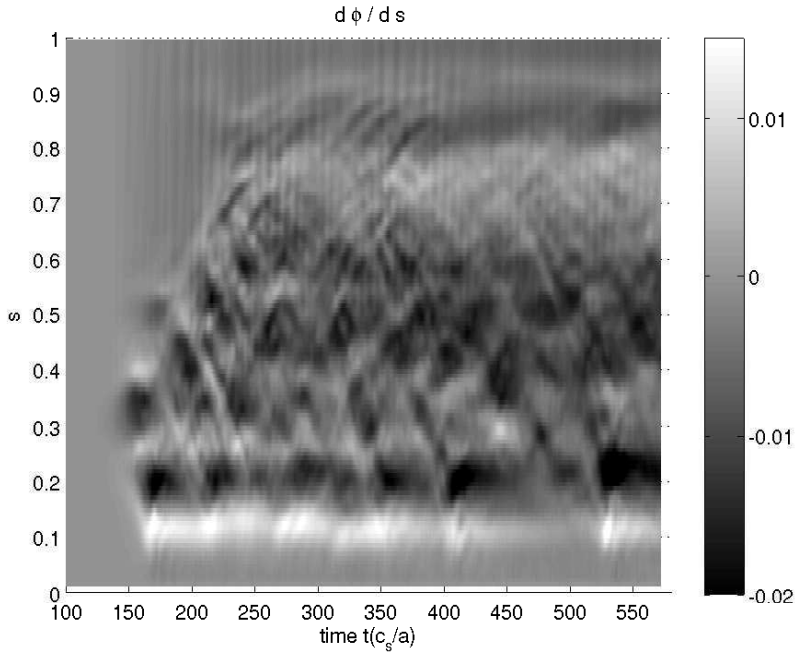

Figure 5: Radial derivative of zonal potential for a $\rho^* = 1/140$ simulation with reduced magnetic shear.

dial dispersion: the dispersion with radial wavenumber might favour propagation in a particular direction, but additional physics seems to be required to fully explain burst propagation.

We have also performed comparisons with the low dimensional models considered in ref. [5] and [6], which we will describe elsewhere. The model of ref. [6] in particular is promising for describing the burst physics. *This work was supported in part by the Swiss National Science Foundation.*

References

[1] S. Jolliet, A. Bottino, P. Angelino, R. Hatzky, T.M. Tran, B.F. McMillan, O. Sauter, K. Appert, Y. Idomura, and L. Villard. A global collisionless PIC code in magnetic coordinates. *Computer Physics Communications*, 177:409–425, 2007.

[2] B. A. Carreras, D. Newman, V. Lynch, and P. H. Diamond. A model realization of self-organized criticality for plasma confinement. *Physics of Plasmas*, 3:2903–2911, 1996.

[3] J. Candy and R. E. Waltz. Anomalous transport scaling in the DIII-D tokamak matched by supercomputer simulation. *Physical Review Letters*, 91:045001, 2003.

[4] T. Dannert and F. Jenko. Gyrokinetic simulation of collisionless trapped-electron mode turbulence. *Physics of Plasmas*, 12:072309, 2005.

[5] Y. Sarazin, X. Garbet, Ph. Grendrih, and S. Benkadda. Transport due to front propagation in tokamaks. *Physics of Plasmas*, 7:1085–1088, 2000.

[6] S. Benkadda, P. Beyer, N. Bian, C. Figarella, O. Garcia, X. Garbet, P. Ghendrih, P. Sarazin, and P.H. Diamond. Bursty transport in tokamak turbulence: Role of zonal flows and internal transport barriers. *Nuclear Fusion*, 41:995–1001, 2001.